Electrochemical studies of gold and chloride in ionic liquids

**Leigh Aldous,[a] Debbie S. Silvester,[b] Constanza Villagrán,[a] William R. Pitner,[c]
Richard G. Compton,[b] M. Cristina Lagunas*[a] and Christopher Hardacre*[a]**

Received (in Montpellier, France) 30th June 2006, Accepted 9th August 2006
First published as an Advance Article on the web 30th August 2006
DOI: 10.1039/b609261f

For the first time, the electrochemistry of gold has been studied in detail in a 'second-generation', non-haloaluminate, ionic liquid. In particular, the electrochemical behaviour of Na[$AuCl_4$] has been investigated in 1-butyl-3-methylimidazolium bis{(tifluoromethyl)sulfonyl}imide, [C_4mim][NTf_2], over gold, platinum and glassy carbon working electrodes. The reduction of [$AuCl_4$]$^-$ initially forms [$AuCl_2$]$^-$ before deposition on the electrode as Au(0). To enable stripping of deposited gold or electrodissolution of bulk gold, the presence of chloride, trichloride or chlorine is required. Specifically trichloride and chlorine have been identified as the active species which preferentially form Au(I) and Au(III), respectively.

Introduction

Ionic liquids (ILs) are defined as salts with melting points of less than 100 °C.[1] As 'liquid salts', ILs display negligible vapour pressures and high ionic conductivities, the latter allowing for their use in electrochemical studies without resorting to the addition of supporting electrolytes. Since most ILs comprise of stable ions, they frequently possess high thermal stability and large electrochemical windows. These, together with the unique solvating abilities of ILs, have led to extensive research into electrochemistry, generally,[2] and, specifically for this study, the redox behaviour of a large range of metals in these solvents.[3–7] Although there are many studies using gold electrodes, these are usually inert (*i.e.*, unless water is present, thus allowing oxide formation), and studies of the electrochemistry of gold compounds in ILs are still sparse.

Ionic liquids incorporating gold into both the anion[4,8] and cation[9] have been prepared, and in the latter, shown to have catalytic activity for the hydration of acetylene.[9] ILs have also been utilised for the preparation and stabilisation of gold nanoparticles,[4,10–16] and Whitehead *et al.* have investigated the quantification of gold in ILs by inductively coupled plasma (ICP) spectroscopy[17] and the 'green' leaching of gold from ore into the IL [C_4mim][HSO_4].[18]

The redox chemistry of gold is dominated by its Au(I) and Au(III) oxidation states, although the Au(I) state is frequently unstable and disproportionates to Au(0) and Au(III).[3] The relative stability of the states and their associated formal redox potentials strongly depend upon both the nature of their ligands and the nature of the solvent.[19]

The electrochemistry of dissolved gold compounds has been studied in chloroaluminate ILs by Xu and Hussey.[3] Therein, an investigation of [$AuCl_4$]$^-$ at a GC electrode was carried out in a Lewis basic aluminium chloride–1-methyl-3-ethylimidazolium chloride ionic liquid. Voltammograms at 40 °C demonstrated two reduction waves at *ca.* +0.10 and −0.70 V (*vs.* Al), corresponding to the reduction of [$AuCl_4$]$^-$ to [$AuCl_2$]$^-$ and its subsequent nucleation and deposition as Au(0), respectively. Following deposition, the oxidative dissolution of the Au deposit was observed at +0.36 V (*vs.* Al), generating [$AuCl_2$]$^-$.

Sun and co-workers studied the electrochemistry of Au(I) at a GC electrode in a Lewis basic 1-methyl-3-ethylimidazolium chloride–tetrafluoroborate ionic liquid, with the reduction of Au(I) and deposition of the metal occurring at −0.52 V, and the anodic stripping to Au(I) at +0.55 V (*vs.* Al).[20] The Au(I) species was introduced into the IL *via* anodic dissolution of an Au substrate at +0.70 V, although the precise nature of the resulting species was not discussed.

Electrochemical investigations using solid crystalline and polycrystalline Au electrodes in ILs are not similarly limited, with the restructuring of Au(111) substrates being investigated in [C_4mim][PF_6][21] and [C_4mPyrr][NTf_2] (1-butyl-1-methylpyrrolidinium bis(trifluoromethylsulfonyl)imide).[22] Harai and co-workers also investigated the surface restructuring of Au(100) in the ILs [C_4mim][BF_4][23] and [C_4mim][NTf_2].[24] In [C_4mim][NTf_2] containing 130 ppm of bromide, a significant oxidative peak with an associated reduction peak were observed prior to the bulk oxidation of the substrate. These were described as corresponding to the oxidation and reduction of gold but were not discussed further.[24]

Gold nanoparticles have been electrodeposited from a mesomorphic IL utilising [$Au(CN)_2$]$^-$ as the anion,[2] although the electrochemical characteristics of this IL were not discussed. Electrodeposition of Al, Sn and Zn on various Au surfaces has also been investigated in basic haloaluminate ionic liquids. In the case of Al, bulk deposition as well as two distinct under-potential deposition regions were identified,[3] whereas deposition of Sn[6] and Zn[7] afforded various alloys. Huang and Sun successfully adapted these observations to form gold deposits with nanosized pores from a 40–60 mol% zinc chloride–1-methyl-3-ethylimidazolium chloride

---

[a] *The QUILL Centre/School of Chemistry and Chemical Engineering, Queen's University, Belfast, Northern Ireland, UK BT9 5AG. E-mail: c.hardacre@qub.ac.uk; Fax: +44 28 9097 4687; Tel: +44 28 9097 4592*
[b] *Physical and Theoretical Chemistry Laboratory, University of Oxford, South Parks Road, Oxford, UK OX1 3QZ*
[c] *Merck KGaA, PLS Ionic Liquids, Frankfurter Strasse, 64271 Darmstadt, Germany*

ionic liquid at 120 °C, initially by the bulk deposition of zinc at −0.2 V (*vs.* Zn) at a polycrystalline Au substrate, then followed by anodic stripping of the surface Au–Zn alloys by applying a potential of +1.0 V (*vs.* Zn).[25] Endres and co-workers have also examined the electrodeposition of metals (*e.g.*, Ge, Ni, Co, Cu, Ag, Al, Si) on Au(111) in both chloroaluminate and non-chloroaluminate ionic liquids.[22,26–31] In the electrodeposition of Al on Au(111) in [C$_4$mim]Cl–AlCl$_3$ formation of Au–Al species were assumed.[27] Similarly, Ge–Au alloys were observed during the electrodeposition of Ge from GeCl$_4$[31] in [C$_4$mim][PF$_6$] whereas using GeBr$_4$ or GeI$_4$ a physical interaction between GeX$_4$ and the gold or of an attack on gold by trace halide was proposed.[28–30]

Gold is known to become unstable and oxidise in positive potential regions, and numerous studies have electrochemically investigated the anodic behaviour of solid gold in aqueous[32] and non-aqueous[3,33,34] media, frequently in the presence of halides. Villagrán *et al.* investigated the electrochemical oxidation of chloride in [C$_4$mim][BF$_4$] and observed its unusual two-step oxidation at an Au electrode, but did not observe any evidence of Au instability or oxidation.[35] Meanwhile, Silvester and Compton have highlighted the effect of trace impurities, including chloride, in the voltammetry of [NTf$_2$]$^-$-based ILs at Au microelectrodes, which give rise to large oxidative peaks attributed to gold oxidation.[36] The mechanism of electrodissolution of gold at the anodic limits in ionic liquids has been examined with *in situ* STM on Au(111) with the oxidation found to start from step sites.[29] Redeposition of gold islands was found close to the open circuit potential (OCP). Furthermore, significant reconstruction of the Au(111) surface was observed at potentials more negative than the OCP in the ionic liquid, [C$_4$mPyrr][NTf$_2$].[22] At the OCP, the surface was rough but became smoother with application of increasingly negative potential showing the mobility of the surface gold atoms under these conditions.

In this work we present the first electrochemical investigation of Na[AuCl$_4$] in a neutral, non-haloaluminate IL, namely [C$_4$mim][NTf$_2$]. We also further explore the rich electrochemistry of chloride in [C$_4$mim][NTf$_2$], highlighting multiple processes at an Au surface leading to multiple oxidation and dissolution routes.

Experimental

Chemical reagents

1-Butyl-3-methylimidazolium chloride ([C$_4$mim]Cl) and 1-butyl-3-methylimidazolium bis{(trifluoromethyl)sulfonyl}imide ([C$_4$mim][NTf$_2$]) were prepared in house using standard literature methods.[1] Sodium tetrachloroaurate dihydrate (Na[AuCl$_4$]·2H$_2$O) (Alfa Aesar) was used as purchased. Tetraethylammonium dichloroaurate ([N$_{2222}$][AuCl$_2$][37]) was prepared using a method analogous to one previously described,[38] which involves the reaction of [AuCl(tht)] (tht = tetrahydrothiophene) with an equimolar amount of [N$_{2222}$]Cl in CH$_2$Cl$_2$. After 2 h, the CH$_2$Cl$_2$ was evaporated, and the resulting precipitate recrystallised three times from CH$_2$Cl$_2$–Et$_2$O. The solid thus obtained was filtered and dried in air (ν_{AuCl} = 348 cm^{-1}). The IL was dried for at least 96 h under high vacuum at 70 °C prior to use. The IL was stored in a N$_2$-filled glove box, and all solutions were prepared in the glove box prior to use.

Instrumentation

Voltammetric experiments were carried out in a 10 cm^3 glass cell with 3 g of ionic liquid. Cyclic voltammogram experiments were recorded with a PC controlled Potentiostat/Galvanostat EG&G Model 273A, and performed with a three-electrode arrangement with a glassy carbon (3 mm diameter), platinum (1.6 mm diameter) or gold (1.6 mm diameter) working electrode, a bright platinum mesh as the counter electrode, and all potentials measured with respect to a 0.01 M Ag$^+$/Ag reference, with AgNO$_3$ dissolved in [C$_4$mim][NO$_3$] and separated from the bulk solution *via* a glass frit. The *iR*-drop was uncompensated. The glassy carbon (GC) electrode was polished using diamond pastes (Kemet, UK) of decreasing particle size (6–0.1 μm) on soft lapping pads. The Au and Pt electrodes were polished with 5 μm, 1 μm and 0.01 μm alumina slurries on lapping pads. All peak assignments for the cyclic voltammograms have been summarised in Table 1.

Electrolysis experiments were carried out in potentiostatic mode in a divided cell (10 cm^3 in volume) using a Potentiostat/Galvanostat EG&G Model 283. A gold wire was used as working electrode, a coiled platinum wire was used as counter and the reference electrode was the 0.01 M Ag$^+$/Ag reference system. A magnetic stirrer was used to stir the contents of the cell throughout the electrolysis. Electrolysis was carried out until the current had decreased from its original value by at least 90%, taking 21–28 h.

Prior to all experiments, the solutions were dried by passing through a column of 4 Å molecular sieves and purged by bubbling argon for at least 10 min. A positive pressure of inert gas was maintained above the surface of the electrolyte throughout the experiments.

Results and discussion

Fig. 1 shows three restricted, cathodic cycles of a 15 mM solution of Na[AuCl$_4$] in [C$_4$mim][NTf$_2$] at a GC electrode. The voltammetric waves I (−0.14 V) and II (−0.75 to −1.20 V) correspond to the two successive reductions, eqn (1) and (2), with both processes releasing chloride into the solution. This assignment is consistent with the cyclic voltammetry of [N$_{2222}$][AuCl$_2$] which, under the same conditions, only showed the presence of peak II. From the plot of peak current *vs.* square-root of scan rate for peak I, the diffusion coefficient of

Table 1 Summary of the proposed reactions and peak assignments

Peak	Proposed reactions
I	$[\text{AuCl}_4]^- + 2\,e^- \rightarrow [\text{AuCl}_2]^- + 2\,\text{Cl}^-$
II	$[\text{AuCl}_2]^- + e^- \rightarrow \text{Au(0)} + 2\,\text{Cl}^-$
III	$3\,\text{Cl}^- \rightarrow \text{Cl}_3{}^- + 2\,e^-$
IV	$\text{Cl}_3{}^- \rightarrow \tfrac{3}{2}\text{Cl}_2 + e^-$
V	$\text{Au}_{(\text{surface})}\text{Cl}^- \rightarrow \text{AuCl}_{(\text{surface})} + e^- \rightarrow$ further oxidative dissolution
VI	$2\,\text{Cl}^- \rightarrow \text{Cl}_2 + 2\,e^-$
VII	Oxidative dissolution by-products
VIII	Oxidative dissolution by-products

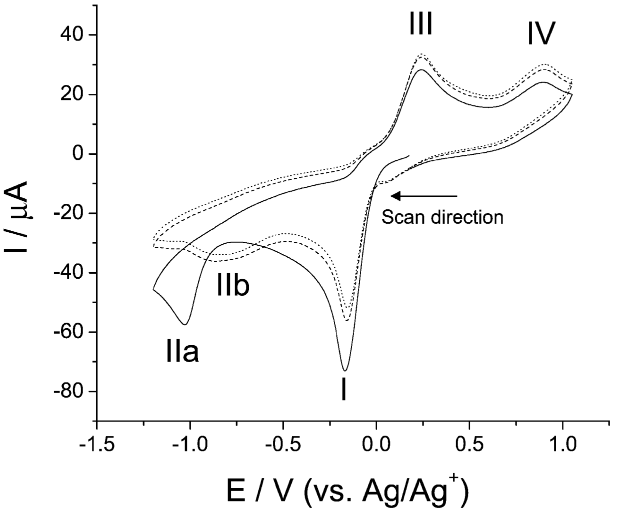

Fig. 1 Cyclic voltammograms of 15 mM of Na[$AuCl_4$] dissolved in [C_4mim][NTf_2] showing the first (—), second (--) and third (···) scans using a GC electrode and a scan rate of 100 mV s^{-1}.

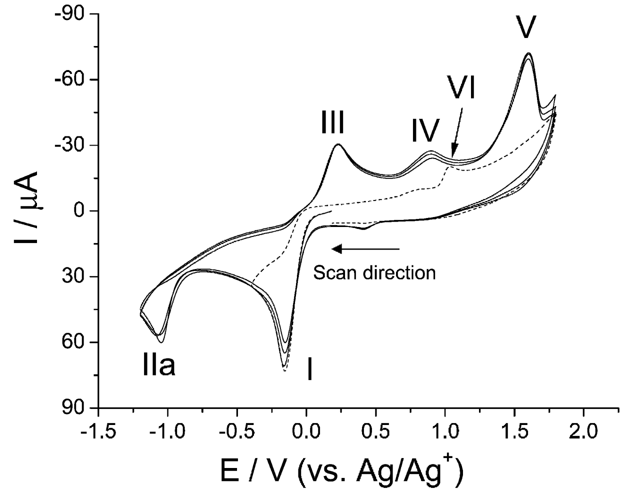

Fig. 2 Cyclic voltammograms of 15 mM of Na[$AuCl_4$] dissolved in [C_4mim][NTf_2] after one restricted (−0.50 V, ···) and three repeated (—) cycles using a GC electrode and a scan rate of 100 mV s^{-1}.

[$AuCl_4$]$^-$ was found to be (5.2 ± 0.5) × 10^{-8} cm^2 s^{-1}.

$$AuCl_4^- + 2e^- \rightarrow AuCl_2^- + 2Cl^- \tag{1}$$

$$AuCl_2^- + 1e^- \rightarrow Au(0) + 2Cl^- \tag{2}$$

With the exception of the deposition feature, II, the cyclic voltammograms were similar on successive cycling. Peak II shifts anodically from −1.05 V in the first cycle, *i.e.* peak IIa, to −0.80 V, peak IIb, with an increase in the breadth of the feature. Initially, the reduction of Au(I) resulted in nucleation and deposition of Au(0) on the GC electrode surface at a potential of −1.05 V. This relatively sharp peak is indicative of the overpotential required for gold nucleation on the GC surface. Nucleation loops were also observed on the return sweep at scan rates of 50 mV s^{-1}, or less, characteristic of diffusion controlled growth continuing at gold nuclei beyond the potential required for the initial nucleation. In subsequent cycles, the reduction of the Au(I) shifts due to the deposition of gold now taking place on active gold deposits supported by the GC electrode.

On the reverse oxidative sweep, two oxidation processes, peak III at +0.23 V and peak IV at +0.89 V, were observed, which are consistent with the two-step oxidation of Cl$^-$ at a gold surface previously described by Villagrán *et al.*[35] Peak III is assigned to the two electron oxidation of chloride to trichloride, eqn (3), whilst peak IV is assigned to its subsequent one electron oxidation to chlorine, eqn (4).

$$3Cl^- \rightarrow Cl_3^- + 2e^- \tag{3}$$

$$Cl_3^- \rightarrow \tfrac{3}{2}Cl_2 + e^- \tag{4}$$

The relative peak currents and areas confirm that processes (3) and (4) are in a 2 : 1 ratio. It is noted that this relative stoichiometry does not support the direct oxidation of Au(0), which would be expected to yield a reverse stoichiometry of 1 : 2, corresponding to Au(0) → Au(I) → Au(III). The observed 2 : 1 process would indicate the formation of a Au(II) intermediate. While these intermediates have been reported, for example, during the reduction of [$AuCl_4$]$^-$ to [$AuCl_2$]$^-$ in CH_2Cl_2,[19] such species are typically difficult to detect and very short lived, and are unlikely to figure prominently in an oxidative electrodissolution process. However, chemical dissolution of Au(0) by the two electrogenerated chloride species cannot be ruled out, as discussed later.

Extending the anodic limit of the reverse cycle to 1.80 V revealed the presence of a third oxidative peak V at *ca.* 1.60 V shown in Fig. 2. This peak was absent if the forward scan was limited to −0.40 V, *i.e.* to include peak I only. In this case only one peak is observed in the reverse scan (*i.e.*, peak VI at +1.04 V; Fig. 2), consistent with the oxidation of Cl$^-$ to Cl_2 at a clean GC surface. Moreover, if the potential is kept above the gold deposition potential, *i.e.* −1.20 V or higher, an increase in peak V on the reverse cycle is found. Repeated cycles at a GC electrode between the gold deposition peak IIa and peak V showed good reproducibility, with negligible shifts in the peak potential of IIa between cycles. This is in contrast with the voltammetry where the anodic limit was reduced so as not to cause gold dissolution *i.e.* peak V, as for Fig. 1, which resulted in the shift in peak II upon repeated cycling. The observed reproducibility is consistent with peak V corresponding to the complete dissolution and removal of gold nuclei from the electrode and thus renewing and maintaining a constant surface for each subsequent scan.

On changing the working electrode to Pt, features I–V were all present, as shown in Fig. 3. While no significant change was observed in the diffusion controlled reduction of Au(III), peak I, the deposition peak on the first cycle, IIa, was observed to shift from −1.05 V on GC to −0.77 V on Pt. This is consistent with the expected lower overpotential required for the nucleation of metal on metal as opposed to metal on GC. Despite the expected strong interaction between gold and platinum, no underpotential deposition of gold was found but this could be masked by peak I. As found with GC, an anodic shift in peak II to −0.60 V, peak IIb, was observed following the first cycle. However, on Pt, this shift was irrespective of whether the scan incorporated the stripping peak V. If the cathodic sweep was

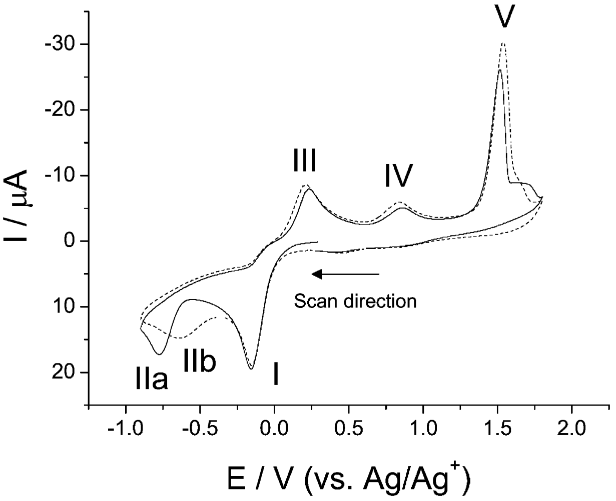

Fig. 3 Cyclic voltammograms of 15 mM of Na[AuCl$_4$] dissolved in [C$_4$mim][NTf$_2$], displaying first (—) and second (--) cycles using a Pt electrode and a scan rate of 100 mV s^{-1}.

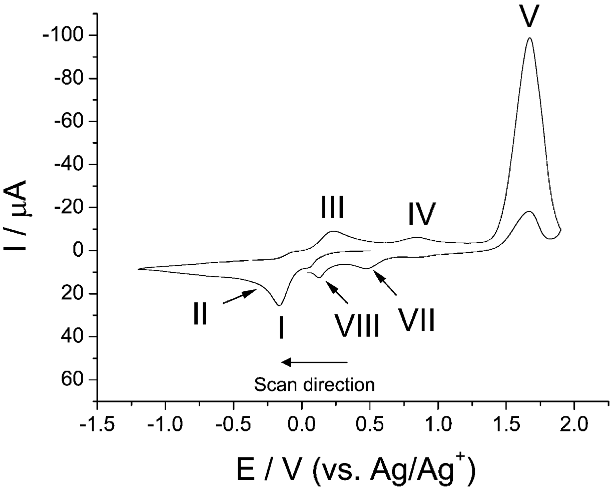

Fig. 5 Cyclic voltammogram of 15 mM of Na[AuCl$_4$] dissolved in [C$_4$mim][NTf$_2$], using an Au electrode and a scan rate of 100 mV s^{-1}.

limited to −0.50 V, *i.e.* to incorporate the formation of [AuCl$_2$]$^-$ (peak I) but not the deposition of gold (peak IIa), a single oxidation peak VI at +1.01 V was observed on the reverse scan (Fig. 4). However, on the second and subsequent cycles, oxidation peaks III and IV are observed as well as an increase in the current at −0.50 V associated with the gold deposition peak IIb. Peak VI is consistent with the oxidation of Cl$^-$ to Cl$_2$ at a clean Pt surface whereas, on subsequent cycles, gold nuclei have been formed thus leading to the gold-related oxidation features, III and IV. This behaviour suggests that the electrochemically formed [AuCl$_2$]$^-$ undergoes disproportionation, eqn (5), with the formation of an active Au(0) layer on the Pt surface. The observation of this disproportionation is highly dependant upon the relative overpotential required for the nucleation of the resulting Au(0), Pt providing a more facile surface for nucleation than GC and thus facilitating disproportionation.

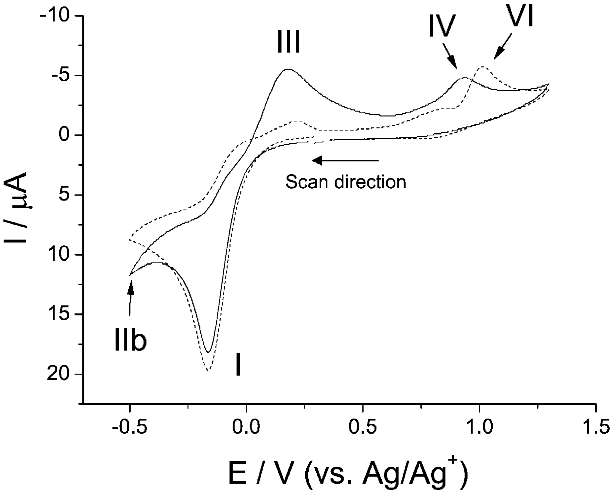

Fig. 4 Cyclic voltammograms of 15 mM of Na[AuCl$_4$] dissolved in [C$_4$mim][NTf$_2$], displaying first (--) and second (—) restricted cycles using a Pt electrode and a scan rate of 100 mV s^{-1}.

$$3\,AuCl_2^- \rightarrow AuCl_4^- + 2\,Au(0) + 2\,Cl^- \qquad (5)$$

The voltammetry of Na[AuCl$_4$] at an Au electrode did not display a well defined deposition peak, with the deposition occurring as a broad unresolved wave after peak I, as shown in Fig. 5. In contrast with the GC and Pt electrode cyclic voltammetry, the dissolution peak V at the Au electrode was large with respect to the amount of Na[AuCl$_4$] reduced and, therefore, the Cl$^-$ released into the vicinity of the electrode. This indicates that dissolution of Au continues beyond the deposited Au layer and continues with extensive dissolution of the gold electrode. In the absence of Na[AuCl$_4$] no dissolution of the electrode is observed and therefore the dissolution is initiated by the presence of halide formed by the reduction of [AuCl$_4$]$^-$. From a comparison of the relative areas of peaks I, II and V,[39] it can be seen that the dissolution of Au at peak V predominantly corresponds to the formation of Au(III), although there is insufficient chloride released to account for the formation of significant concentrations of [AuCl$_4$]$^-$. In addition to peaks I–V, two reductive peaks VII and VIII were observed at +1.47 and +0.13 V, respectively, which were related to peak V. These are thought to correspond to the reduction of Au-intermediates of the dissolution process, or may be related to the restructuring or oxidation of the newly exposed gold surface at the highly positive voltage applied.

A similar process involving the halide-catalysed dissolution of gold has been described in acetonitrile.[33] In this case, it was assumed that a complete monolayer of electrostatically adsorbed halide was responsible for the rapid but limited dissolution of gold. Therein the dissolution was thought to be initiated by the formation of an AuCl surface layer, eqn (6), followed by dissolution of the gold in the form of [AuCl(MeCN)$_n$] with the subsequent catalytic regeneration of Cl$^-$, ultimately yielding solutions of [Au(MeCN)$_{n+1}$]$^+$.[33]

$$Au_{(surface)}Cl^- \rightarrow AuCl_{(surface)} + e^- \qquad (6)$$

The observed chloride-induced oxidation of Au in the [C_4mim][NTf_2] may occur *via* a similar mechanism. In this case the dissolution of $AuCl_{(surface)}$ is likely to be associated with anion complexation *via* binding through the sulfonyl oxygens, eqn (7), as found commonly with transition-metal [NTf_2]$^-$ based complexes.[40] Subsequent oxidation of the [NTf_2]$^-$ based Au complex would yield the expected Au(III) species. This is one possible mechanism and other adsorbed species which could be responsible for the observed gold dissolution include [$AuCl_4$]$^-$.

$$\mathrm{AuCl_{(surface)}} + x\,[\mathrm{NTf_2}]^- \rightarrow \mathrm{AuCl[NTf_2]}_x^{\,x-} \qquad (7)$$

A hysteresis loop, *i.e.* a distinct anodic current peak on the cathodic sweep, was also observed for peak V on the Au electrode at scan rates between 100 and 200 mV s^{-1} (Fig. 5). This may relate to the dissolution of the surface layer of AuCl, or potentially Au[$AuCl_4$], occurring on the timescale of the scan, revealing a clean Au layer below which is in turn rapidly reoxidised.

The direct formation of an Au(III) species during the oxidative dissolution of Au(0) films without the prior and distinct formation of Au(I) is unusual when Au(I) is stable enough to be observed on a reductive scan.[3,19,20,33,34] Commonly, in non-aqueous solvents, oxidation only proceeds as far as the Au(I) state.[3,20,33,34] As a notable exception, Koelle and Laguna[19] observed the two-stage oxidation of Au electrodeposited onto Pt from a solution of PPN[$AuCl_2$] (PPN = bis[bis(triphenylphosphoranylidene)ammonium]) in CH_2Cl_2 in the presence of a large excess of chloride. Therein, the clear oxidation of Au(0) to [$AuCl_2$]$^-$ was followed by the formation of [$AuCl_4$]$^-$ if the anodic limit was extended past the onset of the large Cl^- to Cl_2 oxidative peak.[19] However, it was not possible to confirm that an electrochemical process did in fact overlap with the chloride oxidation process, and so could not rule out a chemical oxidation by reaction with Cl_2.

The nature of the Au-ligands have a distinct effect upon the redox potentials of the Au(I)/Au(0) and Au(III)/Au(I) systems.[19] While the redox potential of the [$AuCl_4$]$^-$/[$AuCl_2$]$^-$ system is clearly positive of the [$AuCl_2$]$^-$/Au(0) system in the IL environment, as evidenced by two distinct reduction processes, similar or negative potential differences during the oxidation process cannot be ruled out if the oxidation species differs from the Au–halide system, *e.g.* [AuCl(NTf_2)]$^-$,[19] such that the Au(III) state becomes more thermodynamically stable than the Au(I) state.

Bis{(trifluoromethyl)sulfonyl}imide anions normally act as chelating ligands through two oxygen atoms, as shown, for example, in the X-ray crystal structure of Zn[NTf_2]$_2$, which forms chains of {Zn[*O*,*O*′-(O_2SCF_3)$_2$N]$_2$} units.[40] This chelating coordination of the [NTf_2]$^-$ would not be expected for Au(I), which preferentially forms two-coordinated linear complexes, but would be compatible with the square-planar coordination preferred by Au(III). The formation of a stable chelated species could be one possible explanation for the observed switch in redox potentials, with oxidative dissolution preferentially forming Au(III) in the [NTf_2]$^-$ system, as distinct from the formation of Au(I) in acetonitrile[33,34] and non-aqueous, chloride-rich solutions.[3,19,20]

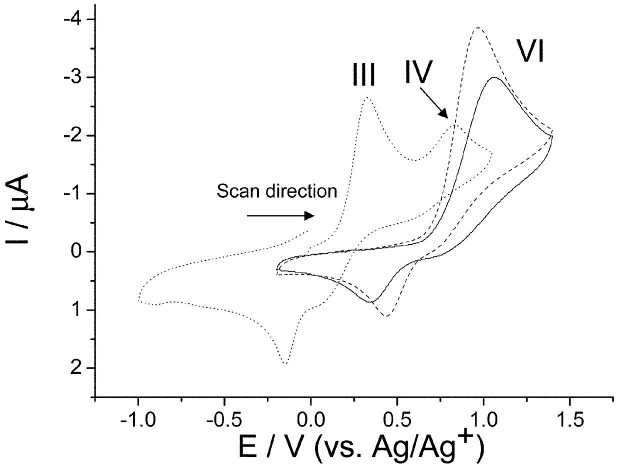

Fig. 6 Cyclic voltammograms of 15 mM of [C_4mim]Cl dissolved in [C_4mim][NTf_2], at Au (···), GC (—) and Pt (--) electrodes, using a scan rate of 100 mV s^{-1}.

In order to verify the speciation of halide and thus the species responsible for the gold dissolution, an investigation of a 15 mM solution of [C_4mim]Cl in [C_4mim][NTf_2] was also carried out. Fig. 6 shows a comparison of the oxidation processes at GC, Pt and Au surfaces (Au dissolution not shown). All oxidative processes, including dissolution, were diffusion controlled processes as demonstrated by linear relationships between the peak current and the square root of the scan rate. The oxidation cycle at the Au electrode showed two irreversible peaks at +0.33 and +0.83 V which compare well with peaks III and IV in Fig. 1–5. These oxidation processes generated a reductive wave and reductive peak at *ca.* +0.10 and −0.15 V, which may be attributed to the reduction of the Cl_3^- and Cl_2 formed *via* reactions (3) and (4), respectively. In contrast, anodic scans using GC or Pt working electrodes displayed only one irreversible oxidative peak for Cl^- at +1.06 or +0.97 V, respectively. The corresponding reduction peaks occurred at +0.34 for GC and +0.45 V for Pt on the subsequent cathodic cycle. This is consistent with the findings of Villagrán *et al.*[35] and Sun *et al.*[41] for voltammetry of chloride in [C_4mim][BF_4] and [C_4mim][PF_6] ionic liquids, respectively.

The voltammetry of chloride on a polished Au electrode displayed cathodic shifts of approximately 0.05–0.15 V for the Cl_3^- formation peak, III, compared with that found on 'deposited-Au' electrodes, *i.e.* formed on GC, Pt or Au electrodes after scanning through the gold deposition peak. In contrast, the potential of the subsequent oxidation of trichloride, peak IV, remained unchanged between different surfaces and subsequent scans. It has been reported that during the aqueous chlorination of suspended gold particles (60–200 μm), adsorption of Cl_3^- was a necessary precursor to an electrochemical oxidation/dissolution sequence ultimately leading to [$AuCl_4$]$^-$.[42] The observed cathodic shift in peak III may therefore be attributed to the increased ease of formation of Cl_3^- facilitated by its adsorption/reaction with nanoscale gold nuclei, *i.e.* with a surface with increased roughness/defects.

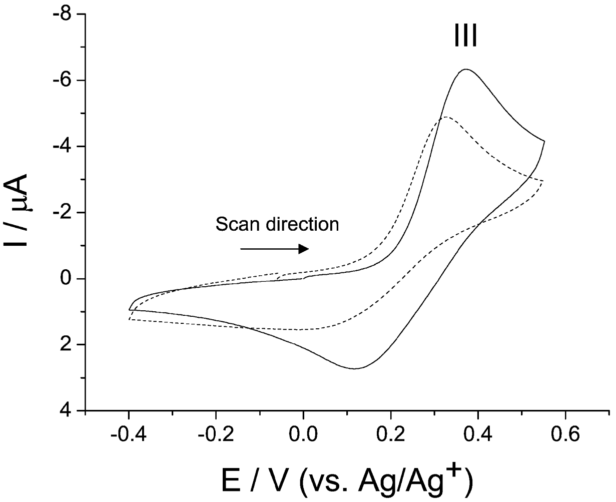

Fig. 7 Cyclic voltammograms of 15 mM of [C_4mim]Cl dissolved in [C_4mim][NTf_2], in the presence (—) and absence (--) of 6.7 × 10^{-4} w/w% H_2O at an Au electrode and a scan rate of 100 mV s^{-1}.

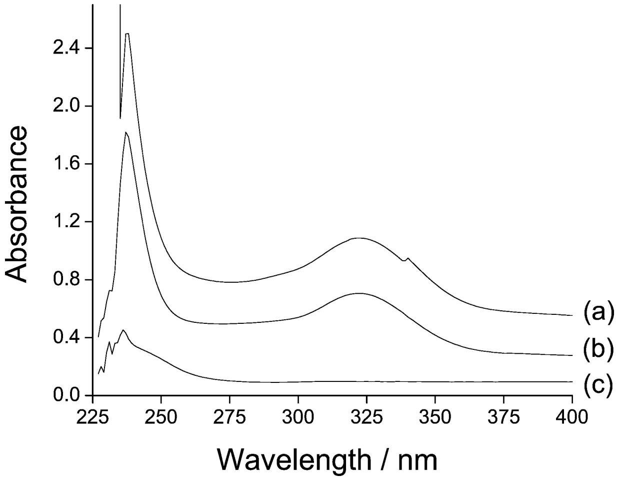

Fig. 8 A comparison of the electronic absorption spectrum of (a) a 20 : 1 dilution of the solution following bulk electrolysis of a gold wire using 100 mM [C_4mim]Cl in [C_4mim][NTf_2] performed at +2.20 V with (b) 0.53 mM Na[$AuCl_4$] dissolved in [C_4mim][NTf_2] and (c) 5.44 mM [N_{2222}][$AuCl_2$] in [C_4mim][NTf_2].

The effect of water on the voltammetry of [C_4mim]Cl in [C_4mim][NTf_2] mixtures was evaluated by the addition of 6.7 × 10^{-4} w/w% H_2O. Over all electrode materials, the addition of water was found to result in an increase in all peak currents, consistent with an increase in conductivity and decrease in viscosity of the system. This has been shown previously by Schröder *et al.* for a range of oxidations and reductions in [BF_4]$^-$ and [PF_6]$^-$ -based imidazolium ionic liquids, for the reduction of cationic methylviologen.[43] The addition of water was also observed to shift the formation of Cl_3^-, peak III, at an Au electrode from +0.33 to +0.37 V, as well as generating a well defined reduction peak at +0.12 V on the cathodic sweep, Fig. 7. In dry ionic liquids, the Cl_3^- would be expected to adsorb at the Au surface and ultimately react with the Au, as described later; however, a passivating layer of adsorbed water, hydroxide or oxide could be responsible for the improved reversibility of the Cl_3^- system. The voltammetry over a glassy carbon electrode was similar in the presence and absence of water, while addition of water improved the reversibility of the Cl_3^- system on Pt, with the separation between oxidation and reduction peaks, ΔE_p, decreasing from 530 mV to 260 mV.

In order to examine the extent of the chloride dependence upon the gold dissolution process V, a gold wire was immersed in a stirred solution of 100 mM [C_4mim]Cl in [C_4mim][NTf_2] and bulk electrolysis was carried out at +2.20 V. This potential was determined by cyclic voltammetry, using the Au wire as working electrode inside the assembled cell, and corresponded to a +0.15 V overpotential relative to the potential of peak V.[44] After an initial sharp decrease in the current from 1.9 to 0.7 mA over the first 10 s of oxidation, the current decreased exponentially without exhaustion or apparent passivation of the Au wire. During the electrolysis, the ionic liquid transformed from colourless to a yellow solution. The electronic absorption spectrum of this solution revealed a broad absorption peak at 322 nm and a sharper, more intense, peak at 238 nm (Fig. 8). This is consistent with the UV-Vis spectrum obtained for Na[$AuCl_4$] dissolved in [C_4mim][NTf_2] indicating the presence of [$AuCl_4$]$^-$. The absorption spectra of [$AuCl_4$]$^-$ in [C_2mim]Cl–$AlCl_3$ was also shown to have a peak at 323 nm.[3] In contrast, a solution of [N_{2222}][$AuCl_2$] in [C_4mim][NTf_2] only showed a series of broad absorption peaks centred at 236 nm. Calibration solutions of Na[$AuCl_4$] in [C_4mim][NTf_2] gave $\varepsilon_{322\,\mathrm{nm}}$ = 4540 ± 290 L cm^{-1} mol^{-1}, which is consistent with the value found for [$AuCl_4$]$^-$ in [C_2mim]Cl–$AlCl_3$ (*i.e.*, $\varepsilon_{323\,\mathrm{nm}}$ = 4600 L cm^{-1} mol^{-1}),[3] and was used to estimate the concentration of [$AuCl_4$]$^-$ in the IL after bulk electrolysis. The total amount of gold in the IL was measured by ICP, and the difference between the two values was assumed to correspond to the presence of [$AuCl_2$]$^-$. Table 2 summarises these results.

Table 2 Speciation and concentration of gold following the bulk electrolysis of a Au wire immersed in a 100 mM [C_4mim]Cl solution in [C_4mim][NTf_2]

Potential applied[a]/V	Concentration Au(I)/mM	Concentration Au(III)/mM	Charge efficiency for total Au dissolved[e] (%)
2.200[b]	0.8	12.9	50.3
1.150[b]	4.4	21.8	95.4
0.600[b]	41.8	1.9	93.9
−0.235[c]	<0.01[d]	<0.01[d]	N/A

[a] Potential *vs.* 0.01 M Ag/Ag^+. [b] With +0.15 V overpotential relative to peak potential at 100 mV s^{-1}. [c] OCP as recorded by potentiostat—initially at −0.200 V which dropped to −0.235 V over the first 60 min. [d] Gold content in solution prior to immersion <0.0037 mM, from ICP. [e] Based on the assumption that the formation of Au(I) and Au(III) occurs *via* one and three electron processes, respectively.

Although electrolysis at +2.20 V clearly leads to a solution predominantly containing $[AuCl_4]^-$ (Table 2), a low charge efficiency of 50.3% was found. Given that the stripping peak occurs close to the onset of the $[NTf_2]^-$ oxidation wave (*i.e.*, the anodic limit of the ionic liquid is marked by the oxidation of the anion at *ca.* +2.0 V), it is likely that the loss of efficiency can be explained by some concurrent oxidation of the ionic liquid. However, Goolsby and Sawyer[34] observed that *complete* reduction of $H[AuCl_4]$ in MeCN at a Pt foil gave an electron count of 2.91 ± 0.03 per Au(III) molecule, while *partial* reduction of $H[AuCl_4]$ solutions gave electron counts as high a five electrons per Au(III) molecule. This was attributed to the presence of stable intermediates, which were only completely reduced by extended electrolysis.[34] Since electrolysis of the Au wire could not be carried to completion, the formation of extensive, undissolved surface intermediates cannot be ruled out.

From the mechanism proposed in eqn (6) and (7), the close agreement between the UV-Vis spectra of the electrolysis solution with that of dissolved $[AuCl_4]^-$ may be surprising. Although the absorption spectrum of $[AuCl(NTf_2)_x]^{x-}$ is not known, it is unlikely to show such a degree of agreement with that of $[AuCl_4]^-$ and therefore its absence is probably due to ligand exchange in solution. Interestingly in MeCN, electrolysis of gold did indicate the presence of $[Au(MeCN)_{n+1}]^+$ albeit where the chloride concentration was 10 000 less than that presented herein.[33] The high concentration of Cl^- used in this study was required due to its depletion by permanent complexation with the gold.

In order to investigate the effect of chloride speciation on the dissolution of gold, bulk electrolysis was carried out at peaks III and IV in 100 mM solutions of $[C_4mim]Cl$ in $[C_4mim][NTf_2]$, in order to generate Cl_3^- and Cl_2, respectively (Table 2). The effect of the chloride anion alone was demonstrated by immersing the gold wire into a stirred 100 mM solution of $[C_4mim]Cl$ in $[C_4mim][NTf_2]$ for 24 h at its OCP. Table 2 also summarises the gold analysis for this experiment. As with bulk electrolysis at +2.20 V, oxidation at +1.15 V, *i.e.* following the formation of Cl_2, was found to yield a clear yellow solution indicating the presence of $[AuCl_4]^-$. In contrast, maintaining the potential at 0.60 V, *i.e.* during the formation of Cl_3^-, the solutions remained largely colourless due to the production of Au(I) primarily, with only slight yellowing being observed consistent with the minor presence of $[AuCl_4]^-$. As expected, by decreasing the potential, the oxidation to Au(I) increased relative to Au(III). Furthermore, both Cl_2 and Cl_3^- systems were found to oxidise Au(0) with >93% charge efficiency, with the concentration of dissolved gold limited only by the initial chloride concentration and speciation of the gold. The solution left at OCP was found to contain a low concentration of Au, indicating only limited corrosion by the Cl^- in the $[NTf_2]^-$ based ionic liquid.

The Cl_2/Cl^- electrolyte system is a well known gold leaching method[45] and it is not unexpected that the generation of Cl_2 in a concentrated Cl^- solution leads to the dissolution of gold in $[C_4mim][NTf_2]$ in the form of $[AuCl_4]^-$; however, the relatively high Au(I) content was surprising. The strongly interlinked reactions between chloride, trichloride and chlorine is one possible explanation for this behaviour.

Sun *et al.*[41] proposed that comproportionation of Cl_2 with excess Cl^- to generate Cl_3^-, eqn (8), can occur in $[C_4mim][PF_6]$.

$$Cl_2 + Cl^- \rightarrow Cl_3^- \qquad (8)$$

The fact that electrolytic formation of Cl_3^- was found to yield a high proportion Au(I), whilst formation of Cl_2 yielded predominantly Au(III) rules out a mechanism of dissolution *via* monochlorination of the Au(0), *e.g.* eqn (9), since this process would yield AuCl and Cl_2 and therefore further oxidation from Au(I) to Au(III) *via* reaction with Cl_2 would be observed.

$$2\,Au(0) + 2\,Cl_3^- \rightarrow 2\,AuCl + 2\,Cl^- + Cl_2 \qquad (9)$$

This mechanism is also not consistent with the fact that dissolution proceeded with 93.9% charge efficiency with respect to the total dissolved Au content, assuming formation of Au(I) is a single electron process. Since the formation of Cl_3^- is a two-electron process, this indicates that each mole of Cl_3^- must oxidise two moles of Au(0), *e.g.* eqn (10).

$$2\,Au(0) + Cl_3^- + Cl^- \rightleftharpoons 2\,AuCl + 2\,Cl^- \rightleftharpoons 2\,AuCl_2^- \qquad (10)$$

The small amount of Au(III) present after the formation of Cl_3^- is likely the result of the formation of Cl_2, either in small quantities during the electrolysis of Cl^- or through the disproportionation described by eqn (8), although disproportionation of the Au(I) species may also occur *via* eqn (5).

Possible causes for the lack of 100% efficiency include the known reactivity of Cl_2 with imidazolium-based ILs.[46] The presence of trace water could also be detrimental, potentially *via* the electrolytic formation of gold oxides at the Au wire surface, or the decomposition of Au(I) to Au(0) prior to quantitative analysis, as previously observed in water–acetonitrile mixtures.[47]

Conclusions

Efficient electrodissolution of gold is demonstrated using a chloride-mediated process in $[C_4mim][NTf_2]$. On examination of the voltammetry of $Na[AuCl_4]$ and chloride in the ionic liquid, it is clear that Au(I) may be preferentially formed using a Cl_3^- process whereas if Cl_2 is used to promote the dissolution, Au(III) is formed. Electrodeposition of gold from dissolved $Na[AuCl_4]$ in $[C_4mim][NTf_2]$ is found to be a two-stage reduction process *via* the formation of $[AuCl_2]^-$.

Acknowledgements

C. V. acknowledges support from QUILL and the School of Chemistry, QUB. L. A. acknowledges support from the Department of Education and Learning in Northern Ireland and Merck KGaA. D. S. S. thanks Schlumberger Cambridge Research for funding *via* a project studentship.

References

1 (*a*) P. Bonhôte, A. P. Dias, N. Papageorgiou, K. Kalyanasundram and M. Grätzel, *Inorg. Chem.*, 1996, **32**, 1168; (*b*) D. R. MacFarlane, P. Meakin, J. Sun, N. Amini and M. Forsyth, *J. Phys. Chem. B*, 1999, **103**, 4164.

2 (*a*) M. C. Buzzeo, R. G. Evans and R. G. Compton, *ChemPhysChem*, 2004, **5**, 1106; (*b*) J. Zhang and A. M. Bond, *Analyst*, 2005, **130**, 1132; (*c*) F. Endres, *ChemPhysChem*, 2002, **3**, 144.

3 X. H. Xu and C. L. Hussey, *J. Electrochem. Soc.*, 1992, **139**, 3103.

4 W. Dobbs, J.-M. Suisse, L. Douce and R. Welter, *Angew. Chem., Int. Ed.*, 2006, **45**, 4179.

5 J.-J. Lee, I. T. Bae, D. A. Scherson, B. Miller and K. A. Wheeler, *J. Electrochem. Soc.*, 2000, **147**, 562.

6 X.-H. Xu and C. L. Hussey, *J. Electrochem. Soc.*, 1993, **140**, 618.

7 W. R. Pitner and C. L. Hussey, *J. Electrochem. Soc.*, 1997, **144**, 3095.

8 M. Hasan, I. V. Kozhevnikov, M. R. H. Siddiqui, A. Steiner and N. Winterton, *Inorg. Chem.*, 1999, **38**, 5637.

9 M. Deetlefs, H. G. Raubenheimer and M. W. Esterhuysen, *Catal. Today*, 2002, **72**, 29.

10 S. Guo, F. Shi, Y. Gu, J. Yang and Y. Deng, *Chem. Lett.*, 2005, **34**, 830.

11 S. Chen, Y. Liu and G. Wu, *Nanotechnology*, 2005, **16**, 2360.

12 Z. Li, Z. Liu, J. Zhang, B. Han, J. Du, Y. Gao and T. Jiang, *J. Phys. Chem. B*, 2005, **109**, 14445.

13 K. Kim, D. Demberelnyamba and H. Lee, *Langmuir*, 2004, **20**, 556.

14 H. Itoh, K. Naka and Y. Chujo, *J. Am. Chem. Soc.*, 2004, **126**, 3026.

15 R. Tatumi and H. Fujihara, *Chem. Commun.*, 2005, 83.

16 L. S. Ott, M. L. Cline, M. Deetlefs, K. R. Seddon and R. G. Finke, *J. Am. Chem. Soc.*, 2005, **127**, 5758.

17 J. A. Whitehead, G. A. Lawrance and A. McCluskey, *Aust. J. Chem.*, 2004, **57**, 151.

18 J. A. Whitehead, G. A. Lawrance and A. McCluskey, *Green Chem.*, 2004, **6**, 313.

19 U. Koelle and A. Laguna, *Inorg. Chim. Acta*, 1999, **290**, 44.

20 F.-Y. Su, J.-F. Huang and I.-W. Sun, *J. Electrochem. Soc.*, 2004, **151**, C811.

21 L. G. Lin, Y. Wang, J. W. Yan, Y. Z. Yuan, J. Xiang and B. W. Mao, *Electrochem. Commun.*, 2003, **5**, 995.

22 N. Borisenko, S. Zein El Abedin and F. Endres, *J. Phys. Chem. B*, 2006, **110**, 6250.

23 K. Kubo, N. Hirai, T. Tanaka and S. Hara, *Surf. Sci.*, 2003, **546**, L785.

24 N. Hirai, T. Yokogawa and T. Tanaka, *Jpn. J. Appl. Phys.*, 2006, **45**, 2295.

25 J.-F. Huang and I.-W. Sun, *Adv. Funct. Mater.*, 2005, **15**, 989.

26 (*a*) S. Zein El Abedin and F. Endres, *ChemPhysChem*, 2006, **7**, 58; (*b*) F. Endres and A. Schweizer, *Phys. Chem. Chem. Phys.*, 2000, **2**, 5455; (*c*) F. Endres, *Electrochem. Solid-State Lett.*, 2002, **5**, C38; (*d*) W. Freyland, C. A. Zell, S. Zein El Abedin and F. Endres, *Electrochim. Acta*, 2003, **48**, 3053.

27 (*a*) C. A. Zell, F. Endres and W. Freyland, *Phys. Chem. Chem. Phys.*, 1999, **1**, 697; (*b*) S. Zein El Abedin, E. M. Moustafa, R. Hempelmann, H. Natter and F. Endres, *Electrochem. Commun.*, 2005, **7**, 1111.

28 F. Endres and C. Schrodt, *Phys. Chem. Chem. Phys.*, 2000, **2**, 5517.

29 F. Endres, *Phys. Chem. Chem. Phys.*, 2001, **3**, 3165.

30 F. Endres and S. Zein El Abedin, *Phys. Chem. Chem. Phys.*, 2002, **4**, 1640.

31 (*a*) F. Endres and S. Zein El Abedin, *Phys. Chem. Chem. Phys.*, 2002, **4**, 1649; (*b*) F. Endres and S. Zein El Abedin, *Chem. Commun.*, 2002, 892.

32 S. Ye, C. Ishibashi, K. Shimazu and K. Uosaki, *J. Electrochem. Soc.*, 1998, **145**, 1614, and references therein.

33 R. Kissner, *J. Electroanal. Chem.*, 1995, **385**, 71.

34 A. Goolsby and D. T. Sawyer, *Anal. Chem.*, 1968, **13**, 1978.

35 C. Villagrán, C. E. Banks, C. Hardacre and R. G. Compton, *Anal. Chem.*, 2004, **76**, 1998.

36 (*a*) D. S. Silvester and R. G. Compton, *Z. Phys. Chem.*, 2006, submitted; (*b*) D. S. Silvester and R. G. Compton, unpublished results.

37 P. Braunstein and R. J. H. Clark, *J. Chem. Soc., Dalton Trans.*, 1973, 1845.

38 J. Vicente, M. T. Chicote and M. C. Lagunas, *Inorg. Chem.*, 1993, **32**, 3748.

39 Representative examples of the peak areas taken at a scan rate of 100 mV s^{-1} on a GC electrode are I = 119.0 μC, II = 58.2 μC, V = 153.0 μC, giving a ratio for I : II : V of 2.0 : 1.0 : 2.6; on a platinum electrode I = 17.3 μC, II = 8.3 μC, V = 29.6 μC, giving a ratio of 2.1 : 1.0 : 3.6; and on a gold electrode I + II = 31.4 μC, V = *ca.* 245 μC giving a ratio of 3.0 : 23.4.

40 M. J. Earle, U. Hakala, B. J. McAuley, M. Nieuwenhuyzen, A, Ramani and K. R. Seddon, *Chem. Commun.*, 2004, 1368.

41 H. Sun, L. Yu, X. Jin, X. Hu, D. Wang and G. Chen, *Electrochem. Commun.*, 2005, **7**, 685.

42 J. Vinals, C. Nunez and O. Herreros, *Hydrometallurgy*, 1995, **38**, 125.

43 U. Schröder, J. D. Wadhawan, R. G. Compton, F. Marken, P. A. Z. Suarez, C. S. Consorti, R. F. de Souza and J. Dupont, *New J. Chem.*, 2000, 1009.

44 Note, a difference in peak potential was observed for peak V using the planar Au macroelectrode compared with the gold coiled wire in the divided cell setup used for bulk electrolysis. In the former the potential was +1.7 V whereas for the electrolysis setup a voltage of +2.05 V was found which corresponds to the 150 mV overpotential with respect to the electrolysis potential of +2.20 V.

45 M. A. Diaz, G. H. Kelsall and N. J. Welham, *J. Electroanal. Chem.*, 1993, **361**, 25.

46 (*a*) N. Winterton, K. R. Seddon and Y. Patell, *World Pat.*, WO 0037400, 2000; (*b*) F. M. Donahue, J. A. Levisky, G. F. Reynolds and J. S. Wilkes, *J. Electrochem. Soc.*, 1985, **132**, 372C.

47 R. Kissner, G. Welti and G. Geier, *J. Chem. Soc., Dalton Trans.*, 1997, 1773.